Slip Deficit Rates Estimation at Baribis Fault on 2016-2019 GPS Observations

Fikri Z. Fuadi*, Henri Kuncoro, Sidik T. Wibowo, Aditya Rizqiansyah

Geodetic Engineering, Faculty of civil engineering and planning, Institut Teknologi Nasional (Itenas)Bandung
Badan Informasi Geospasial (BIG)

ABSTRACT

The surrounding area Baribis-Kendeng Fault is featured by active tectonic deformation. The slip deficit rate distribution is essential in explaining seismo-tectonics and assessing the risk of seismic hazards in this area because Java Island is the most populous island in the world. In this study, we collect GPS data from CORS stations and TPG stations then process the original carrier phase data of GPS to obtain the consistent velocity field in the ITRF2014. We assume two blocks separated by the Baribis fault: the Sunda block (footwall) and the Java block (hangingwall). The obtained velocity vector is used to estimate the Euler rotation parameter of each block. The estimated Euler poles parameters of the Java and Sunda blocks are estimated as their locations at 20.9° N, 120.2° E and 63.3° N, 112.2° W, respectively, and their angular velocities of 0.511°/ Myr counter-clockwise and 0.263°/ Myr counter-clockwise. These parameters produce Baribis fault slip rates with 3 mm/yr with strike fault in all segments. The slip deficit rates distribution is characterized by fully locking in the Subang 1 segment in the depth range from 10-20 km with the rate of 0.8 - 1 mm/yr.

Keywords: Baribis Fault, Slip Rates, Slip Deficit Rates, ITRF2014, Euler Rotation

1. Introduction

Java Island is located at the junction between the Sunda Plate and Indo Australia, where there is a subduction zone situated in the south of West Java. Several faults were formed to accommodate stress generated by Java subduction [1]. One of the faults formed as a result of the stress is the Baribis Fault. The Baribis Fault Zone is one of the major fault zones in the western part of Java Island where follows the Java Pattern. The Baribis fault is an active fault that contributed to the Majalengka earthquake in 1990. The Baribis fault extends from east to west in the West Java region. Based on the results of Marliyani's study (2016), the Baribis Fault is a fault zone consisting of several segments that have different fault mechanisms in every segment. Tampomas segment, Cirebon segment, Brebes segment is a reverse fault, and Ciremai segment is a strike-slip fault [2]. In the Baribis fault, there are three segments monitored by the Geospatial Information Agency (BIG) with campaign station Geodynamic Monitoring Point (TPG), which is in the Subang 1 segment, Subang 2 segment, and Ciremai segment (Figure 1).

GPS observation data is used in numerical modeling by involves the kinematic calculation of block geometry models defined in two different blocks. We used continuous GPS data for the past three years to model the fault deformation by combining rigid block motion and fault slip deficit.

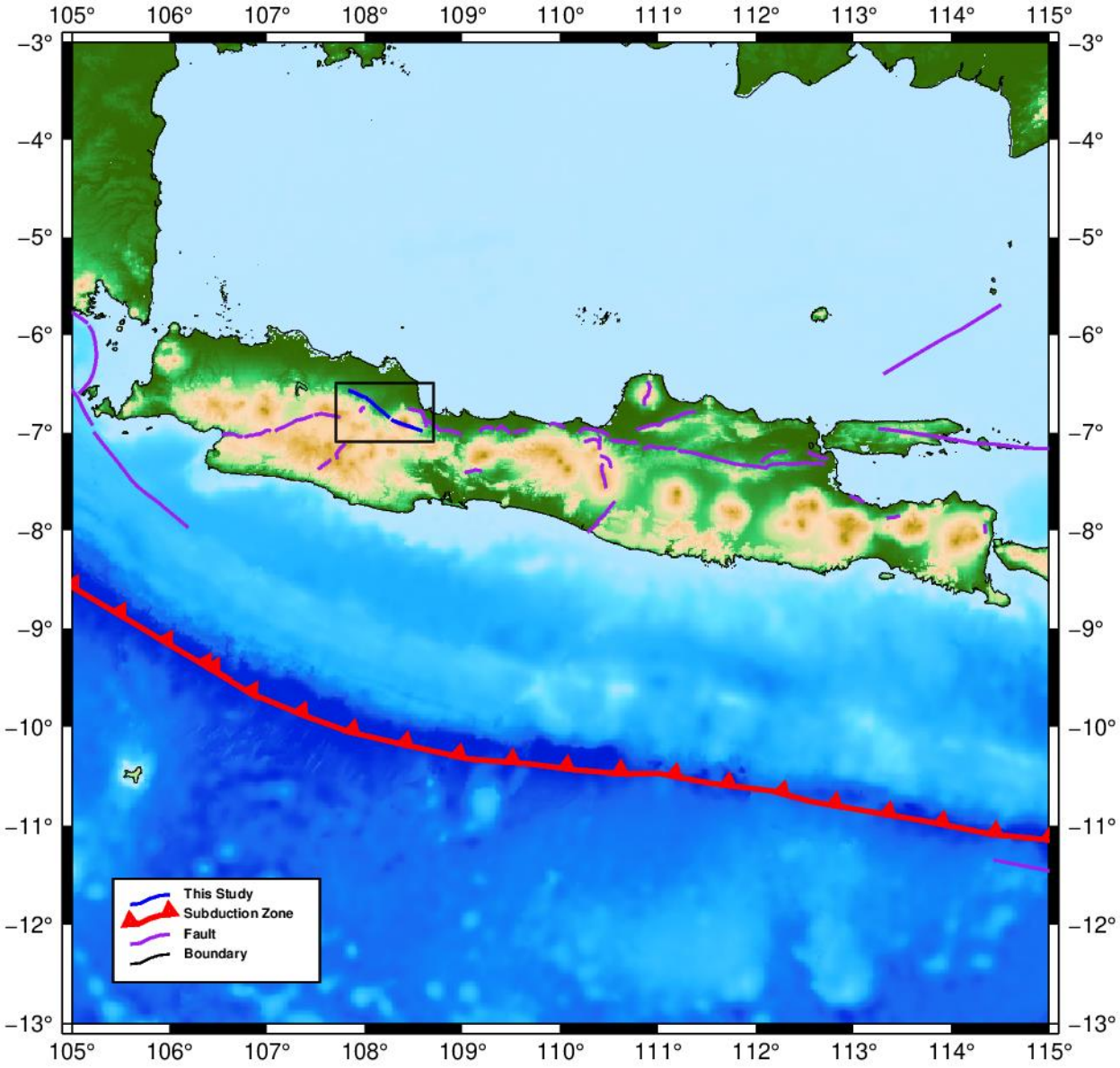

Fig. 1. Tectonic map in Java Island. Red lines show the subduction zone, purple lines show the active faults. Blue lines in the black boundary show Baribis Segments in this study.

The elastic component of deformation is proportional to the slip deficit on each fault segment, so a fully creeping segment generates no elastic deformation. In Indonesia, slip deficit rate research is only for sea faults or subduction zones. There is no slip deficit rates research on land faults in Indonesia, especially at Baribis Fault. Therefore, the purpose of this study to estimate the slip deficit rate of Baribis Fault. The slip deficit rate distribution is essential to explain seismo-tectonics and assess the risk of seismic hazards in this area because Java Island is the most populous island. Thus, this study is expected to provide deformation information at the Baribis Fault to be used as a disaster mitigation effort.

2. Data and Method

2.1 GPS data and processing

Our study's GPS observations were obtained from the continuous network and campaign station of Badan Informasi Geospasial (BIG) from 2016 to 2019. The GPS velocity field presented in this study is calculated from observations at 42 Indonesia Continuously Operating Reference Station (Ina-CORS) located in Kalimantan Island, Natuna Besar Island, Belitung Island, and Java Island along 18 campaign station of Geodynamic Monitoring Point (TPG) in combination with a global network of 18 International Global Navigation Satellite Systems Service (IGS) tracking sites. The results of the GPS position time series may be affected by the subduction zone. Since the subduction effect is difficult to correct because of its complexity, to reduce the subduction effect's influence on the velocity fields, we exclude GPS data from Southern Java for reducing the subduction effect.

We processed these data using the GAMIT/GLOBK software (version 10.7) [3]. We estimated the loosely-constrained positions by including 18 IGS stations, and then we obtained solutions using the Kalman Filter (GLOBK) to derive a consistent set of positions and velocities. Velocity fields can be estimated using the least-squares method, where that is the line gradient of the time series. A linear model can be estimated from the time series by fitting all data in a time interval. Mathematically, the linear model is obtained from the following equation [4]:

$$[y]_A = m[x]_A + b \tag{1}$$

Where y is a matrix that contains the value of the displacement at station A (north, east, or up), x is the epoch matrix of observations at station A, m is the line's slope, and b is a constant. To estimate realistic uncertainties and account for noise in the GPS time series, we have used a first-order Gauss Markov extrapolation (FOGMEX) algorithm [5].

In addition to the velocity, velocity precision is also estimated using the parameter variance-covariance equation [6]:

$$\Sigma_{xx} = \hat{\sigma}^2 \times (A^T P A)^{-1} \tag{2}$$

whit $\hat{\sigma}^2$ (a posteriori variance) is:

$$\hat{\sigma}^2 = \frac{V^T V P}{n-u} \tag{3}$$

Where *V* is the residual observation matrix (V = AX - L), *P* is the weight matrix, *n* is the number of observations, and *u* is the number of parameters. Thus, the precision of moving velocity is the square root of the variance or the diagonal of the variance-covariance matrix parameters [6].

2.2 Modeling of Block Rotation

In the book Earthquake and Volcano Deformation written by Seagall (2010), Euler's Theorem defines a small change from a defined position on a plate uniquely described based on an axis's rotation. Euler's rotation parameters are defined by Euler's poles in latitude and longitude (λ and φ) and angular velocity of rotation (ω), assuming that the earth is spherical. Euler's rotation parameter is estimated from the angular rotation on the x, y, and z axes [6]. Then the angular rotation vector is estimated using the equation [7] as follows:

$$\begin{bmatrix} V_n \\ V_e \\ V_u \end{bmatrix} = \begin{bmatrix} -\sin\varphi\cos\lambda & -\sin\varphi\sin\lambda & \cos\varphi \\ -\sin\lambda & \cos\lambda & 0 \\ \cos\varphi\cos\lambda & \cos\varphi\sin\lambda & \sin\varphi \end{bmatrix} \begin{bmatrix} 0 & Z & -Y \\ -Z & 0 & X \\ Y & -X & 0 \end{bmatrix} \begin{bmatrix} \omega_X \\ \omega_Y \\ \omega_Z \end{bmatrix} \quad (4)$$

Then can be estimated the Euler's poles parameters (λ, φ) and the angular velocity (ω) as follows [6]:

$$\varphi = tan^{-1}\left(\frac{\omega_Z}{\sqrt{\omega_X{}^2 + \omega_Y{}^2}}\right)$$
$$\lambda = tan^{-1}\left(\frac{\omega_Y}{\omega_X}\right)$$
$$\omega = \sqrt{\omega_X{}^2 + \omega_Y{}^2 + \omega_Z{}^2} \quad (5)$$

Block rotation is estimated based on Euler's rotation parameter. This is represented by the velocity models whose estimation process is called forward calculation. We used block modeling to estimate the velocity models [8]. The Euler's poles parameter is given a strict constraint as big as its standard deviation to estimate the velocity models with the block modeling. This is intended so that Euler's poles parameter's value does not change when the forward calculation is carried out. Then the angular rotation vector is used to estimate the velocity models. A forward calculation can be done to calculate the velocity of the Euler's poles parameters by re-estimating the angular rotation in the spherical coordinate system using [6]:

$$\omega_X = acos(\varphi)\, cos(\lambda)$$
$$\omega_Y = acos(\varphi)\, sin(\lambda)$$
$$\omega_Z = asin(\varphi) \quad (6)$$

2.3 Slip Deficit Rates Calculation

The linear horizontal velocity of a point in block *i* relative to the reference frame *R* is ${}_R\boldsymbol{V}_i = {}_R\boldsymbol{\Omega}_i \times \boldsymbol{X}$ where *X* is the vector from the center of the earth to the surface point (λ, ϕ) where the velocity is estimated. The difference in linear velocity of the two blocks calculated from Euler's poles at the fault points is called the slip rates. The slip rates on the fault that separates block *i* and *j* at point *X* are [9]:

$$ {}_j\boldsymbol{V}_i = {}_R\mathbf{V}_i - {}_R\mathbf{V}_j \tag{7}$$

Some parts of the slip rates on faults do not occur constantly, usually referred to as fault locking. The calculation of slip rates in this study uses TDEFNODE software. This software applies the Savage [10] back-slip method using Okada's [11] formulas to compute surface velocities around locked faults embedded in a homogeneous, elastic half-space. Because the velocities due to Euler rotations are calculated in spherical coordinates, and plate locking velocities are typically calculated in Cartesian coordinates, we assume that $V_x = V_e$ and $V_y = V_n$. It should be noted that the surface deformation due to the fault interactions can be calculated with any appropriate method, and the material need not be fully elastic [9].

The fault locking is represented by slip deficit rates $-\phi.V$, where ϕ is a coupling ratio at each node and estimated by the code, and *V* is the fault slip rates. The coupling ratio ϕ assures that the fault slip rate and slip deficit rate are kinematically consistent with block rotations. If $\phi = 0$, then the fault is freely slipping (creep), and if $\phi = 1$, then the fault is fully locked. if $0 < \phi < 1$ then partial locking occurs. In inversion, ϕ is kept between -1 and 1 [1].

3. Result

3.1 Block Rotation

The GPS velocity field can directly reflect the Sunda Block and the Jawa Block overall movement. Fig.2 shows that the station velocity in Sunda Block and Java Block decreases to the southeast, indicating that the Sunda Block's extrusion leading to Java Block. To obtain the detailed kinematic characteristics in the Sunda Block and Java Block, 21 GPS stations distributed across the Sunda Block and Java Block were selected for calculating their Euler vectors. The Euler vectors were estimated to be 63.332° N, 112.193° W, 0.263°/Myr for Sunda Block, and 20.897° N, 120,235° E, 0.511°/Myr for Java Block. Fig.3 shows that the majority of the velocity models are exact with the observed velocity. The precision indicates that the model velocity vector is quite good at representing the Sunda block and the Java block movement. The velocity models' quality can be seen through the residual value obtained from the Euler's poles parameter estimation. The residual value is obtained from the difference between the observed velocity and the velocity model for each GPS observation station.

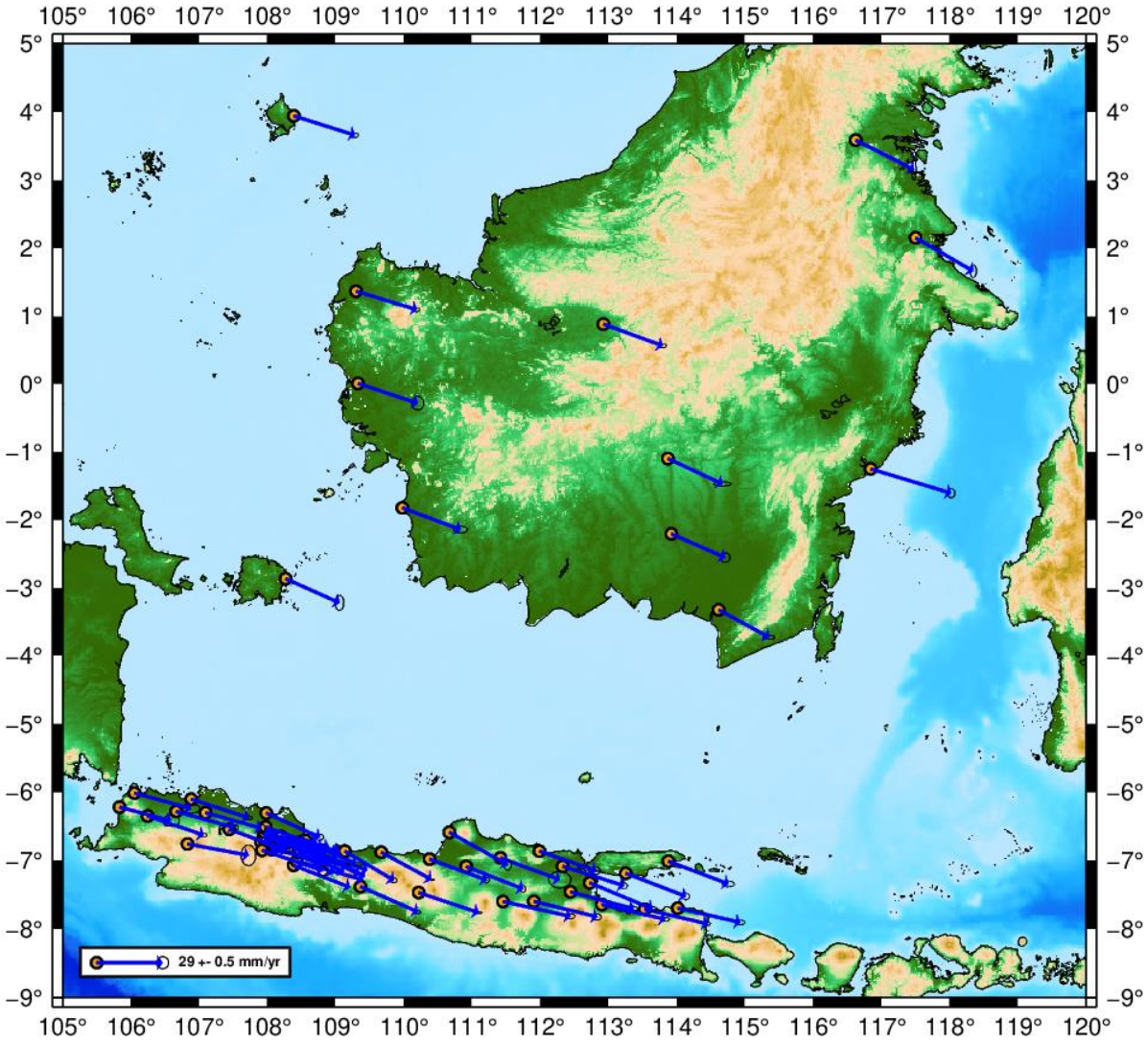

Fig. 2. Velocity vectors map. Blue vectors indicate the movement vector with the error ellipse indicated on a scale of 0.5 mm/yr.

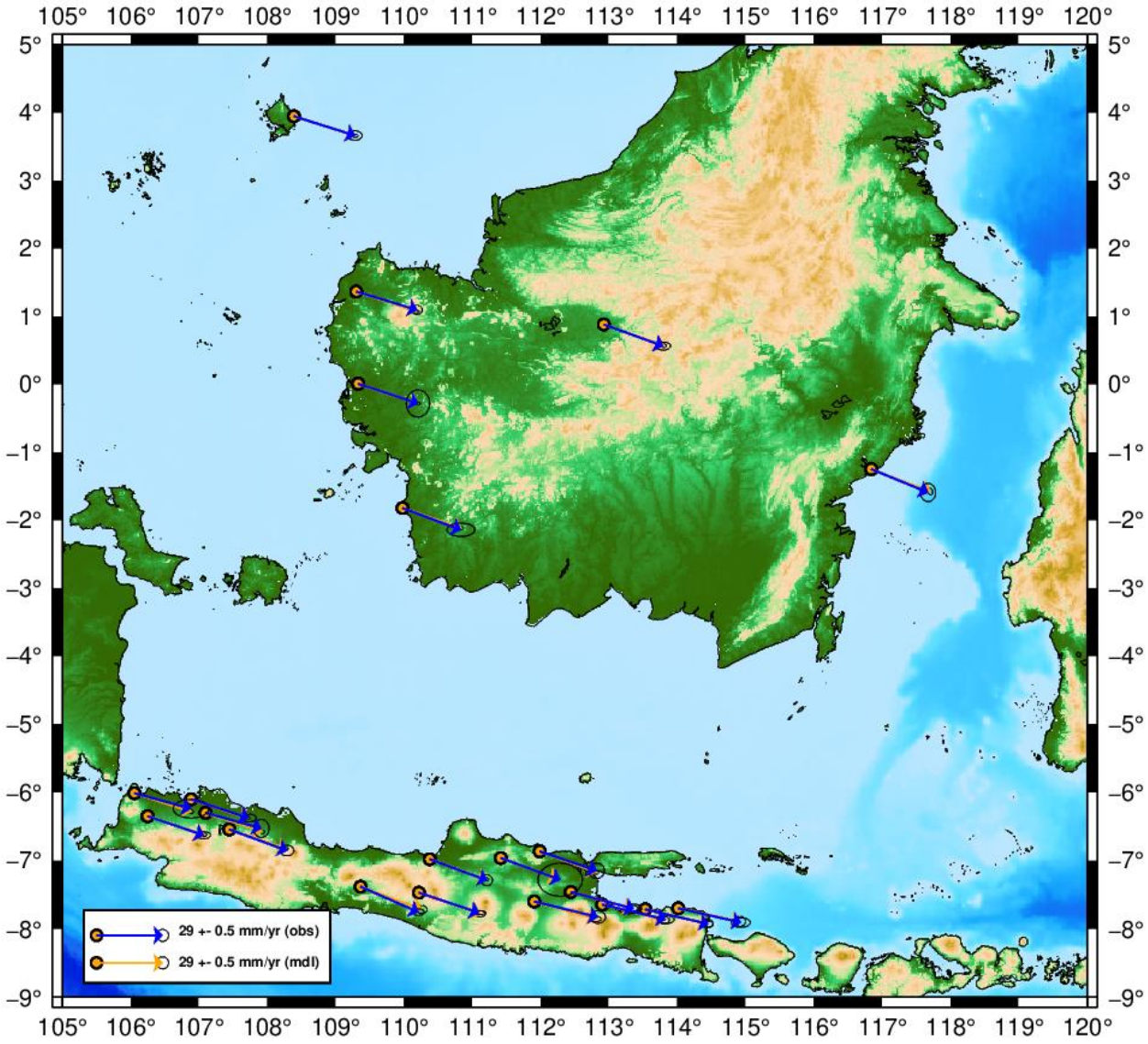

Fig. 3. The precision between the modeled velocity vector and the observed velocity vector. Blue vectors show the observed velocity vector. Yellow vectors show the modeled velocity vector.

3.2 Slip Rates on Baribis Fault

In the slip rates estimation, 21 GPS stations were used, such as estimating the Euler rotation parameter and the Euler rotation parameter. We apply the Savage [10] back-slip method using Okada's [11] formulas to estimate Baribis Fault slip rates. Fig.4 shows all of these segments leads to the southeast, where the slip rate is 3 mm/yr.

The results of elastic locking modeling on the Subang 1 segment have slip rates of 3.2 mm/yr with a strike of 2.3 mm/yr and a thrust of 2.2 m /yr, for the Subang 2 segment have slip rates of 3.0 mm/yr with a strike of 2.8 mm/yr, and a thrust is 1.1 mm/yr, and slip rates for the Ciremai segment have slip rates of 2.8 mm/yr with a strike value of 2.3 mm/yr and thrust of 1.6 mm/yr (Figure 5).

4. Discussion

4.1 Characteristic of Baribis Fault

The deformation phenomenon in the Baribis Fault can be analyzed from the residual velocity vector of movement. After the block rotation effect is removed, several large residuals have a particular deformation pattern. Fig.6 shows the residual velocity vector in Kalimantan Island with a value of 0.084-1.130 mm/yr is caused by intrablock deformation due to the movement of local faults in this area. While among faults that extend northern of Java Island, include the Baribis Fault, 0.332 - 1.875 mm/yr residual velocity vector leads to the north and south, meaning that the fault extending north of Java Island, including the Baribis Fault, occurs the elastic deformation phenomenon.

Strike rate is more dominant than the thrust rate in all segments, this shows that the segment it is a shear-strike fault. Fig.5 shown that the Baribis fault contains an earthquake with a depth of below 100 km, indicating that the earthquake may have occurred due to the Baribis Fault activity. The slip vector generated from the focal mechanism shows the opposite direction to the slip rate. This could be due to the influence of southern Java subduction, and the GPS data used in this study does not represent the Sunda Block, so the slip rate is directed towards the southwest of Java Island.

4.2 Interplate Coupling Baribis Fault

In this study, three velocity vectors of the CORS station and 18 velocity vectors of the TPG Baribis fault were used to estimate slip deficit rates because the steady secular deformation is distributed fairly uniformly over regions extending up to 100 km from Baribis Fault [12].

Fig.7 shows that the distribution of slip deficit rates is shown by fully locking in the Subang 1 segment (Profile A-B) at 10-20 km depth with slip deficit rates 0.8 - 1 mm/yr. Subang 1 indicates that this segment can produce earthquakes soon as happened in 2000 (M5.0). In the Subang 2 segment (Profile C-D) at 20 km depth, there is partial locking with slip deficit rates of less than 0.8 mm/yr, this indicates that Subang 2 segment can produce earthquakes but not soon, even though there is no earthquake history. The Ciremai segment (Profile E-F) does not show locking, and this may be due to an earthquake in 1990 (M5.5), which made the segment not produce locking.

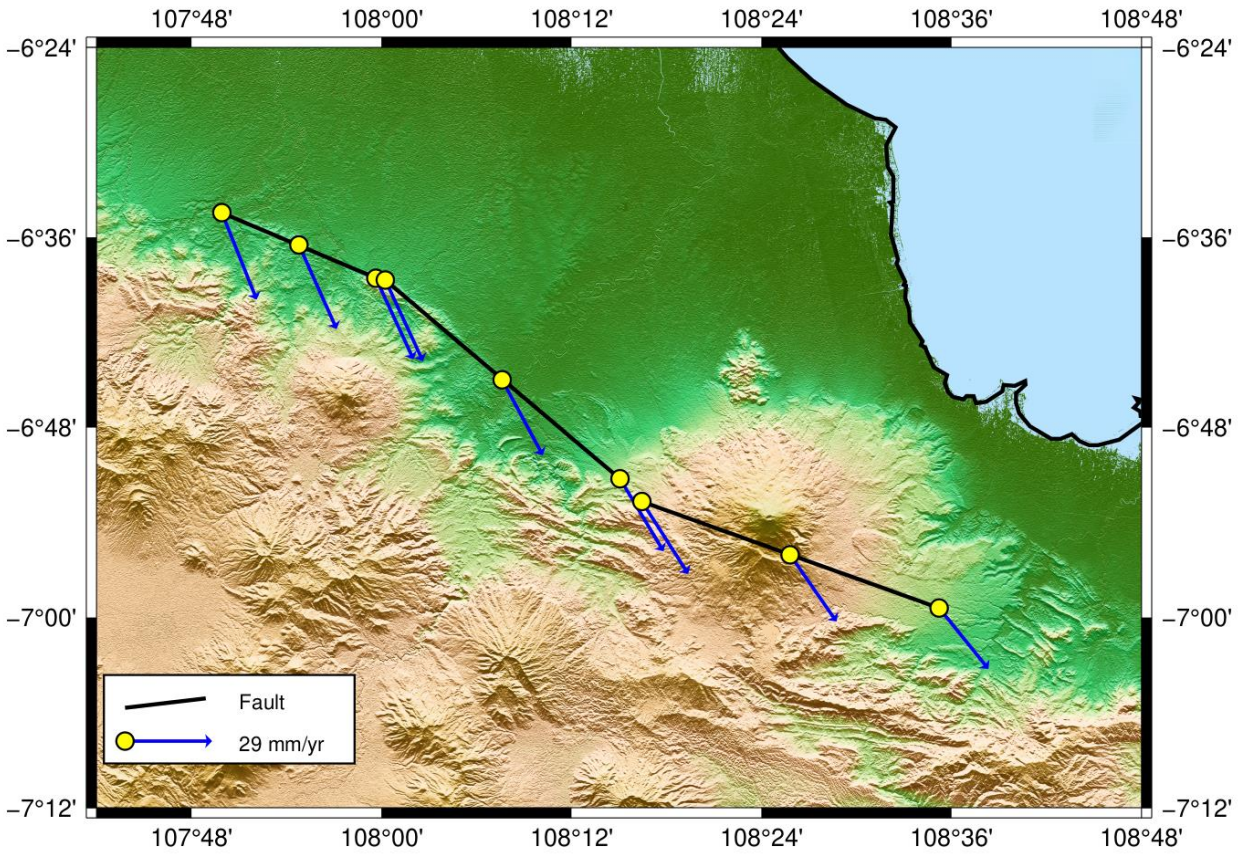

Fig. 4. Fault slip rate vectors. The black lines show generalized fault segments. Blue vectors with a yellow circle show slip rate vectors.

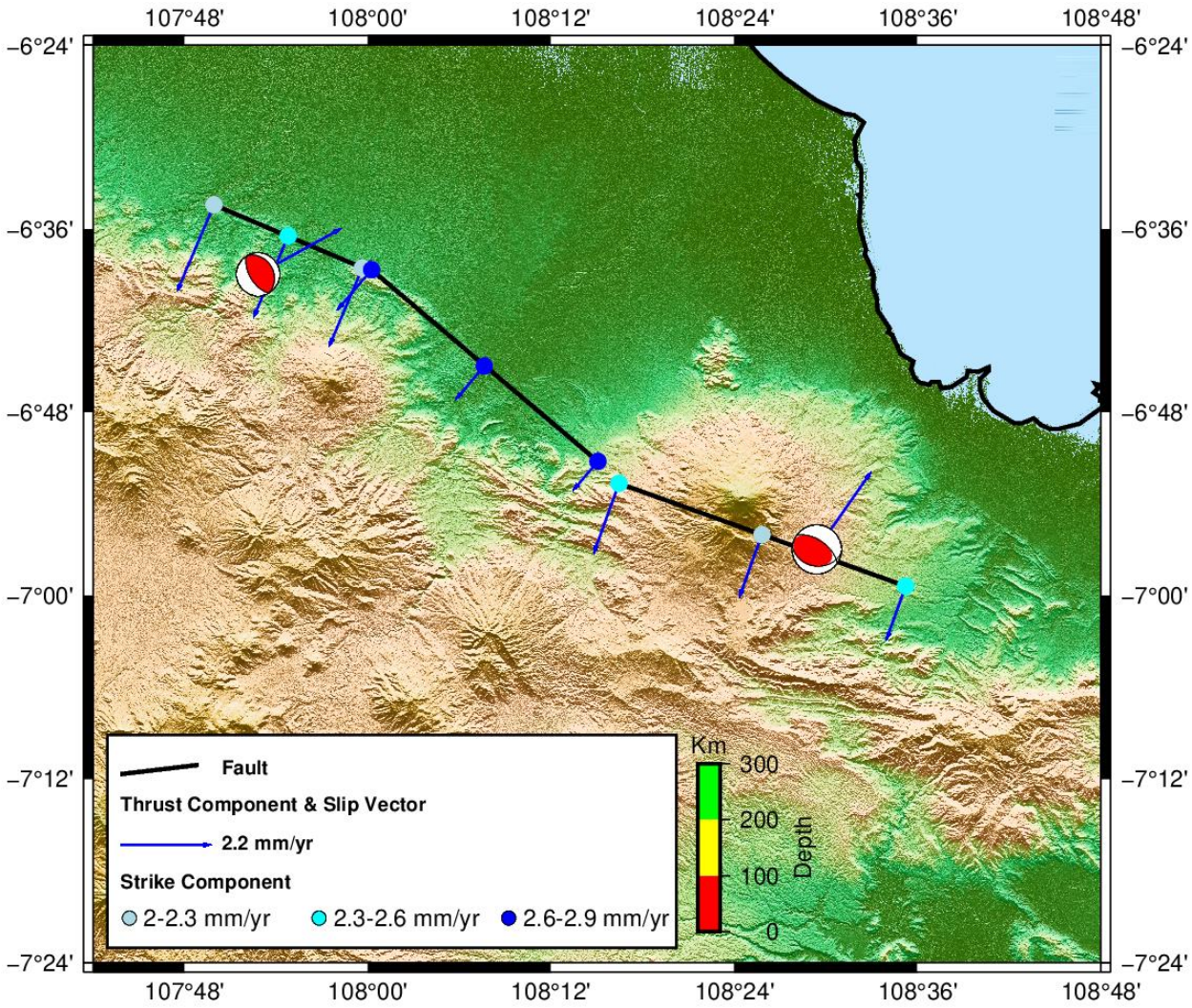

Fig.5. Fault slip rates, focal mechanism, and slip vectors. The black lines show generalized fault segments. Blue vectors show thrust component vectors and slip vectors. Cyan, light blue, and dark blue circles show strike component.

5. Conclusion

A combination of the campaign and continuous GPS observations in Kalimantan and Java shows block rotation and elastic deformation in the Baribis Fault. This study's results are the distribution of slip deficit rates and deformation conditions in the Baribis Fault.

Estimated Euler's poles parameters indicate a location at 63.332° N, 112.193° W, with an angular velocity of 0.263°/Myr counter-clockwise for the Sunda Block and 20.897° N, 120,235° E, with an angular velocity of 0.511°/Myr counter-clockwise for the Java Block. These parameters produce slip rates in the Baribis Fault with a value of about 3 mm / yr with two reverse fault segments in the Subang 1 and Ciremai segments and the strike fault segments in the Subang 2 segment.

The distribution of slip deficit rates is shown by fully locking in the Subang 1 segment (Profile A-B) at 10-20 km depth with slip deficit rates of 0.8 - 1 mm/yr. Subang 1 indicates this segment can produce earthquakes soon as happened in 2000 (M5.0). In the Subang 2 segment (Profile C-D) at 20 km depth, there is partial locking with slip deficit rates of less than 0.8 mm/yr, this indicates that Subang 2 segment can produce earthquakes but not soon, even though there is no earthquake history. The Ciremai segment (Profile E-F) does not show locking, and this may be due to an earthquake in 1990 (M5.5), which made the segment not produce locking.

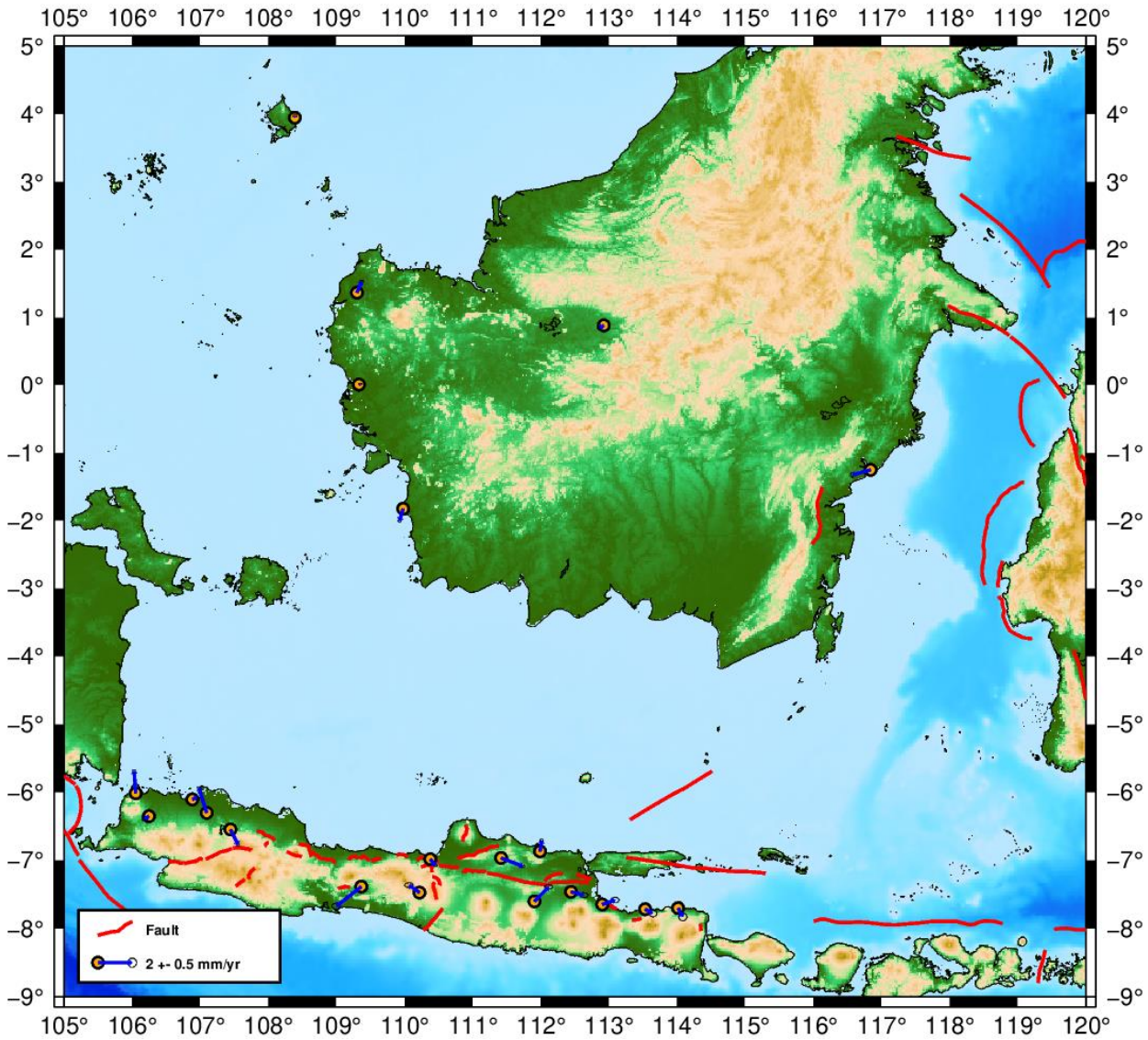

Fig. 6. Residual vectors. Red lines show the active Fault. Blue vectors with a yellow circle show the residual vectors.

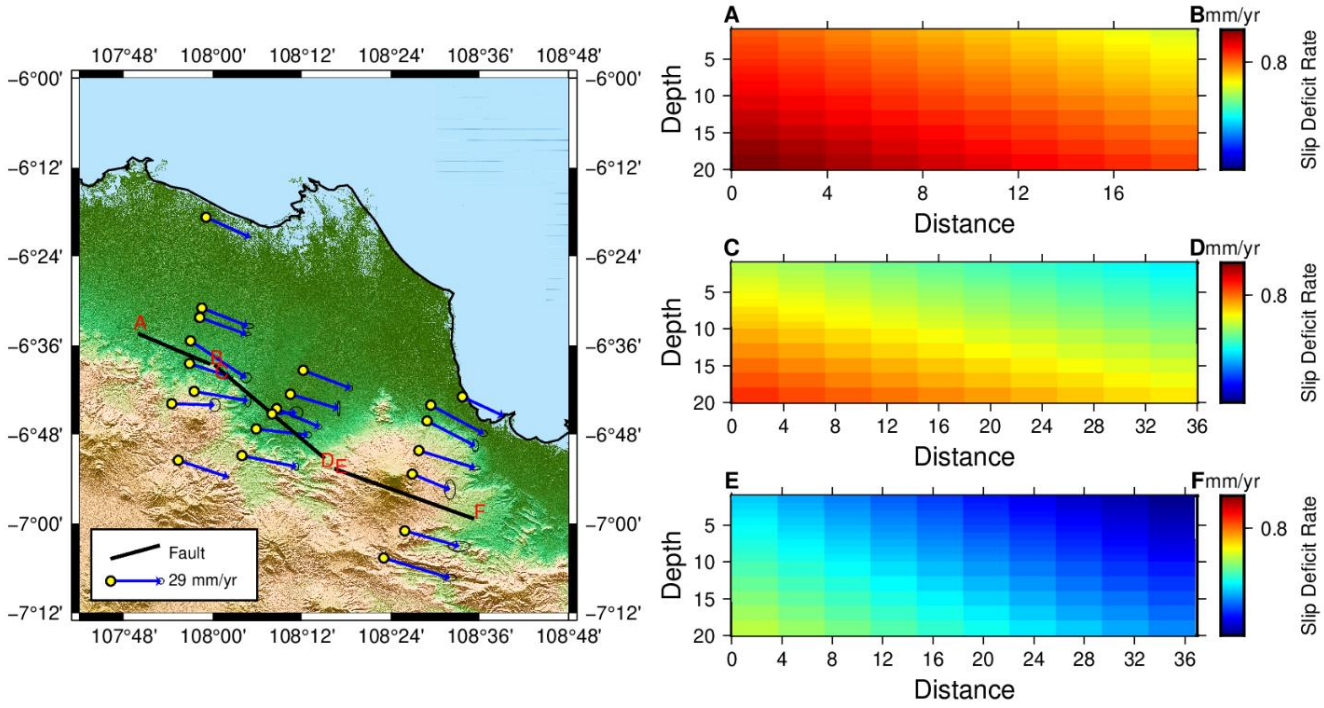

Fig. 7. **S**lip deficit rates distribution. The black lines show generalized fault segments (profile). Blue vectors show velocity vectors. Profile A-B, C-D, and E-F show the slip deficit distribution.

Reference

[1] H. Kuncoro, "Rotation of the Sunda block and spatiotemporal characteristics of the interplate coupling in the Java subduction zone, Indonesia," *Tohoku Univ.*, 2018.

[2] Pusgen, *Buku Peta Gempa 2017*. 2017.

[3] T. A. Herring, R. W. King, M. A. Floyd, S. C. Mcclusky, and P. Sciences, "Introduction to GAMIT/GLOBK Release 10.7," no. June, pp. 1–168, 2018.

[4] P. R. Wolf and C. . Ghilani, *Adjustment Computations: Spatial Data Analysis*. 2006.

[5] T. A. Herring, M. A. Floyd, R. W. King, and S. C. Mc Clusky, "GLOBK Reference Manual," no. June, pp. 1–95, 2015, [Online]. Available: http://geoweb.mit.edu/gg/GLOBK_Ref.pdf.

[6] H. Kuncoro, "Methodology of Euler Rotation Parameter Estimation Using GPS Observation Data," vol. 1, no. 2, pp. 42–55, 2013.

[7] S. Cox and R. Hart, *Plate Tectonics: How it Works*. Oxford: Blackwell Publishing, 1986.

[8] B. J. Meade and J. P. Loveless, "Block modeling with connected fault-network geometries and a linear elastic coupling estimator in spherical coordinates," *Bull. Seismol. Soc. Am.*, vol. 99, no. 6, pp. 3124–3139, 2009, doi: 10.1785/0120090088.

[9] R. Mccaffrey, "Crustal Block Rotation and Plate Coupling," *Plate Bound. Zo.*, 2002, doi: 10.1029/GD030p0101.

[10] J. C. Savage, "A dislocation model of strain accumulation and release at a subduction zone," *J. Geophys. Res.*, vol. 88, pp. 4984–4996, 1983.

[11] Y. Okada, "Surface deformation to shear and tensile faults in a half-space," *Bull. Seism. Soc. Am.*, vol. 75, pp. 1135–1154, 1985.

[12] W. Thatcher, "Horizontal crustal deformation from historic geodetic measurements in Southern California," *J. Geophys. Res. Solid Earth*, vol. 84, no. B5, pp. 2351–2370, 1979, doi: 10.1029/JB084iB05p02351.